

WEAK LENSING STUDY OF GALAXY BIASING

HENK HOEKSTRA,^{1,2,3} LUDOVIC VAN WAERBEKE,^{1,4} MICHAEL D. GLADDERS,^{2,3,5} YANNICK MELLIER,^{3,4,6} AND H. K. C. YEE^{2,3}
Received 2002 February 18; accepted 2002 June 8

ABSTRACT

We combine weak lensing measurements from the Red-Sequence Cluster Survey (RCS) and the VIRMOS-DESCART survey and present the first direct measurements of the bias parameter b and the galaxy-mass cross-correlation coefficient r on scales ranging from 0.2 to $9.3 h_{50}^{-1}$ Mpc (which correspond to aperture radii of $1'5-45'$) at a lens redshift $z \simeq 0.35$. We find strong evidence that both b and r change with scale for our sample of lens galaxies ($19.5 < R_C < 21$), which have luminosities around L_* . For the currently favored cosmology ($\Omega_m = 0.3$, $\Omega_\Lambda = 0.7$), we find $b = 0.71^{+0.06}_{-0.04}$ (68% confidence) on a scale of $1-2 h_{50}^{-1}$ Mpc, increasing to ~ 1 on larger scales. The value of r has only minimal dependence on the assumed cosmology. The variation of r with scale is very similar to that of b and reaches a minimum value of $r \sim 0.57^{+0.08}_{-0.07}$ (at $1 h_{50}^{-1}$ Mpc; 68% confidence). This suggests significant stochastic biasing and/or nonlinear biasing. On scales larger than $\sim 4 h_{50}^{-1}$ Mpc, the value of r is consistent with a value of $r = 1$. In addition, we use RCS data alone to measure the ratio b/r on scale ranging from 0.15 to $12.5 h_{50}^{-1}$ Mpc ($1'-60'$) and find that the ratio varies somewhat with scale. We obtain an average value of $b/r = 1.090 \pm 0.035$, in good agreement with previous estimates. A (future) careful comparison of our results with models of galaxy formation can provide unique constraints, as r is linked intimately to the details of galaxy formation.

Subject headings: cosmology: observations — dark matter — gravitational lensing

1. INTRODUCTION

The growth of structures in the universe via gravitational instability is an important ingredient in our understanding of galaxy formation. However, the connection to observations is not straightforward, as we need to understand the relation between the dark matter distribution and the galaxies themselves. Galaxy formation is a complex process, and it is not guaranteed a priori that this relation, referred to as galaxy biasing, is a simple one. The bias might be nonlinear, scale dependent, or stochastic. In the simplest case, linear deterministic biasing, the relation between the dark matter and the galaxies can be characterized by a single number, b (Kaiser 1987).

Most observational constraints of biasing come from dynamical studies (see Strauss & Willick 1995) which probe relatively large scales ($10 h_{50}^{-1}$ Mpc or more). Recent estimates on these scales suggest values of $b \sim 1$ for L_* galaxies (e.g., Peacock et al. 2001; Verde et al. 2001). On smaller scales, some constraints come from measurements of the galaxy two-point correlation function, which is compared to the (dark) matter correlation function computed from numerical simulations. These studies indicate that the bias parameter $b \simeq 0.7$ on scales less than $\sim 2 h_{50}^{-1}$ Mpc ($\Omega_m = 0.3$, $\Omega_\Lambda = 0.7$). On larger scales, b increases to a value close to unity (Jenkins et al. 1998).

Although this procedure provides useful information about the bias parameter b as a function of scale, it does rely on the assumptions made in the numerical simulations. In addition, it cannot be used to examine the tightness of the correlation between the matter and light distribution. To determine that, we need to measure the galaxy-mass cross-correlation coefficient r , which is a measure of the amount of stochastic and nonlinear biasing (e.g., Pen 1998; Dekel & Lahav 1999; Somerville et al. 2001).

The coherent distortions in the shapes of distant galaxies caused by weak gravitational lensing provide a unique way to study the dark matter distribution in the universe. Weak lensing probes the dark matter distribution directly, regardless of the light distribution. In addition, it provides measurements on scales from the quasi-linear to the nonlinear regime, where comparisons between observations and predictions are still limited. Much progress has been made in recent years, and the latest results give accurate joint constraints on the matter density Ω_m and the normalization of the power spectrum σ_8 (e.g., Bacon et al. 2002; Hoekstra et al. 2002b; Refregier, Rhodes, & Groth 2002; van Waerbeke et al. 2002).

Although redshift surveys can be used to determine the relative values of b and r for different galaxy types (Tegmark & Bromley 1999; Blanton 2000), weak gravitational lensing provides the only direct way to measure the galaxy-mass cross-correlation function (Fischer et al. 2000; Wilson, Kaiser, & Luppino 2001; McKay et al. 2001; Hoekstra, Yee, & Gladders 2001b). Fischer et al. (2000) used the Sloan Digital Sky Survey commissioning data to measure the galaxy-mass correlation function, and their results suggested an average value of $b/r \sim 1$ on submegaparsec scales. This approach has been explored by Guzik & Seljak (2001), who used semi-analytic models of galaxy formation combined with N -body simulations. Their results suggest that the cross-correlation coefficient is close to unity. The galaxies used in their analysis, however, are massive (and consequently luminous) because of the limited mass resolution of the simulations.

¹ CITA, University of Toronto, Toronto, ON M5S 3H8, Canada.

² Department of Astronomy and Astrophysics, University of Toronto, Toronto, ON M5S 3H8, Canada.

³ Visiting Astronomer, Canada-France-Hawaii Telescope, operated by the National Research Council of Canada, Le Centre National de Recherche Scientifique, and the University of Hawaii.

⁴ Institut d'Astrophysique de Paris, 98 bis Boulevard Arago, 75014 Paris, France.

⁵ Current address: Observatories of the Carnegie Institution of Washington, 813 Santa Barbara Street, Pasadena, CA 91101.

⁶ Observatoire de Paris, LERMA, 61 Avenue de l'Observatoire, 75014 Paris, France.

In this paper, we use the method proposed by Schneider (1998) and van Waerbeke (1998), which allows us to measure the biasing parameters directly as a function of scale. Hoekstra, Yee, & Gladders (2001a) applied this technique to 16 deg² of R_C -band imaging data from the Red-Sequence Cluster Survey (RCS; e.g., Yee & Gladders 2001) and measured the ratio b/r as a function of scale. They found an average value of $b/r = 1.05^{+0.12}_{-0.10}$ for a Λ CDM cosmology on scales ranging from $150 h_{50}^{-1}$ kpc to $3 h_{50}^{-1}$ Mpc.

However, an accurate measurement of the mass autocorrelation function is required to constrain b and r separately. Furthermore, the analysis is facilitated if the measurements of both the galaxy autocorrelation function and the mass autocorrelation function probe the power spectrum at the same redshift. To this end, the measurements presented by van Waerbeke et al. (2002), based on deep imaging data from the VIRMOS-DESCART survey, are ideal. In this paper, we combine the results of the RCS and the VIRMOS-DESCART survey, allowing us to measure both b and r as a function of scale for the first time.

The structure of the paper is as follows. In § 2, we discuss the data sets we use for our analysis. In § 3, we define the bias parameters and show how they can be related to observed correlation functions. The relevant correlation functions are discussed in § 4. The actual measurements are discussed in § 5. The inferred bias parameters are presented in § 6. In the Appendix, we demonstrate that the method used in this paper gives accurate results if the bias parameters vary with scale and redshift.

2. DATA

The Red-Sequence Cluster Survey⁷ is a galaxy cluster survey designed to provide a large number of clusters with $0.1 < z < 1.4$ (Yee & Gladders 2001). Here we use the R_C -band data from the northern half of the survey, which consists of 10 widely separated patches on the sky, observed with the CFH12k camera on the Canada-France-Hawaii Telescope (CFHT). The total area observed is 45.5 deg², but because of masking, the effective area is somewhat smaller, with a total of 42 deg² used in the lensing analysis. The data and weak lensing analysis are described in detail in Hoekstra et al. (2002a).

The VIRMOS-DESCART survey⁸ consists of four patches in four colors also observed with the CFHT12k camera. The final survey will cover 16 deg², but here we use 8.5 deg² of I -band data described in van Waerbeke et al. (2001).

These data have been used elsewhere to derive joint constraints on Ω_m and σ_8 using the weak lensing signal caused by large-scale structure (Hoekstra et al. 2002a, 2002b; Pen et al. 2002; van Waerbeke et al. 2001, 2002). These papers describe in detail the object detection, the shape measurements, and the corrections for the various observational distortions (point-spread function anisotropy, seeing, and camera shear). These studies have shown that the contamination of the lensing signal by residual systematics is small.

The accuracy of the measurement of the galaxy autocorrelation function increases with survey area, and hence the

RCS data are best suited for this measurement. Currently, the VIRMOS-DESCART survey provides the most accurate measurement of the mass autocorrelation function (in particular, on scales less than 10'), although the RCS data also provide useful constraints on cosmological parameters (Hoekstra et al. 2002b). On scales less than 10', the accuracy of the RCS measurements is likely limited by intrinsic alignments of the sources, whereas the VIRMOS-DESCART measurements do not suffer from this. For the galaxy-mass cross-correlation function, we use the results from the RCS because the lenses used for the determination of the galaxy autocorrelation function were selected from this survey.

Currently, we do not have redshift information for the RCS galaxies, and we, therefore, select a sample of lenses on the basis of their apparent R_C -band magnitude: we define a sample of lenses from the RCS with $19.5 < R_C < 21$, which yields a total of $\sim 1.2 \times 10^5$ lenses. For the measurement of the galaxy-mass cross-correlation function, we use source galaxies with $21.5 < R_C < 24$, which yield $\sim 1.5 \times 10^6$ sources. The weak lensing analysis of the VIRMOS-DESCART data uses $\sim 5 \times 10^5$ galaxies with $I_{AB} < 24.5$.

In order to interpret the measurements, we have to know the redshift distributions of the lens galaxies and the two populations of source galaxies. The CNOC2 Field Galaxy Redshift Survey (Yee et al. 2000) has determined the redshift distribution of galaxies down to a nominal limit of $R_C = 21.5$. Hence, the results from CNOC2 provide an excellent measure of the redshift distribution of our sample of lenses ($19.5 < R_C < 21$), for which we obtain a median redshift of $z = 0.35$.

The source galaxies from the RCS and the VIRMOS-DESCART surveys have different redshift distributions, and these galaxies are generally too faint for spectroscopic surveys. Fortunately, photometric redshifts work well, as demonstrated by Hoekstra, Franx, & Kuijken (2000). We use photometric redshift distributions derived from both Hubble Deep Fields (Fernández-Soto, Lanzetta, & Yahil 1999) and multicolor observations done with the Very Large Telescope (van Waerbeke et al. 2002). We find a median redshift of $z = 0.53$ for the RCS source galaxies (with $21.5 < R_C < 24$). The galaxies from the VIRMOS-DESCART survey are fainter, and the selection of galaxies with $I_{AB} < 24.5$ gives a median redshift of $z \simeq 0.9$. Although the source redshift distributions are quite different, we will show below that the two surveys are actually well matched, as both probe the power spectrum at $z \sim 0.35$ (see Fig. 1).

3. METHOD

To study the galaxy biasing, we use a combination of the galaxy and mass autocorrelation functions as well as the cross-correlation function. The statistic we use to present the results is the aperture mass, M_{ap} , which is described in detail in Schneider et al. (1998). It is defined as (Kaiser et al. 1994)

$$M_{ap}(\theta) = \int d^2\phi U(\phi)\kappa(\phi), \quad (1)$$

where κ is the dimensionless surface density. Provided $U(\phi)$ is a compensated filter, i.e., $\int d\phi\phi U(\phi) = 0$, with $U(\phi) = 0$ for $\phi > \theta$, the aperture mass can be expressed in term of the observable tangential shear γ_t using a different filter func-

⁷ Go to <http://www.astro.utoronto.ca/~gladders/RCS>.

⁸ Go to <http://www.astrsp-mrs.fr/virmos/> and <http://terapix.iap.fr/Descart/>.

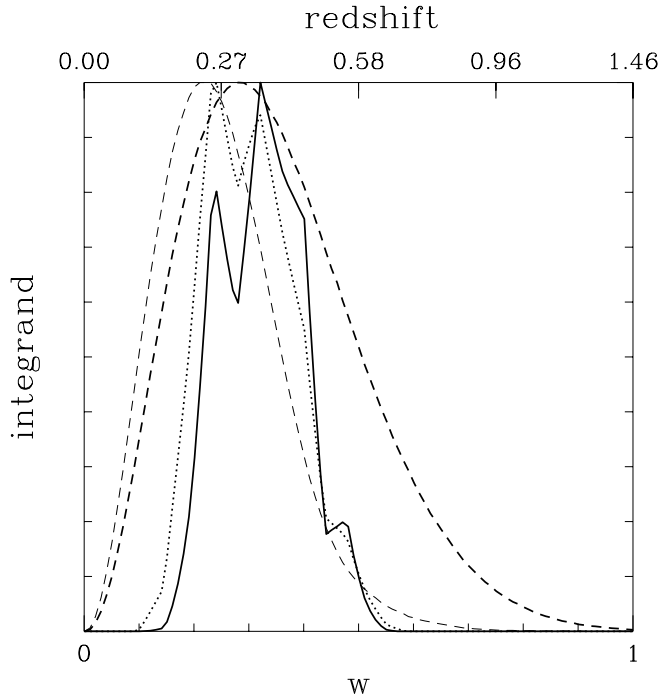


FIG. 1.—Different integrands of the integrals in eqs. (14) and (17) for a fiducial aperture size $\theta_{\text{ap}} = 5'$. The integrands have been normalized to have the same maximum value. *Thick solid line:* $h_1(w)$ as a function of w . *Upper axis:* Corresponding redshift. We used the observed redshift distribution of galaxies with $19.5 < R_C < 21$ from the CNOC2 survey, which gives rise to the wiggles in the function. This result indicates that we probe the power spectrum (and the bias parameters) at an effective redshift ~ 0.35 . *Thick dashed line:* $h_2(w)$ for the VIRMOS-DESCART survey. This function is rather broad, which reflects the fact that weak lensing probes the power spectrum over a relatively large redshift range. However, comparison with the integrand for the galaxy autocorrelation function shows that both peak at the same redshift. Hence, we can use the ratio of $\langle \mathcal{N}^2 \rangle$ and $\langle M_{\text{ap}}^2 \rangle$ measured at the same aperture size θ_{ap} . The same integrand using the RCS background galaxy redshift distribution gives the thin dashed line, which is a poor match to galaxy autocorrelation function. *Dotted line:* Integrand for the galaxy-mass cross-correlation function, $h_3(w)$, which overlaps well with the galaxy autocorrelation function.

tion $Q(\phi)$ [which is a function of $U(\phi)$],

$$M_{\text{ap}}(\theta) = \int_0^\theta d^2\phi Q(\phi) \gamma_t(\phi). \quad (2)$$

We use the filter function suggested by Schneider et al. (1998),

$$U(\phi) = \frac{9}{\pi\theta_{\text{ap}}^2} \left[1 - \left(\frac{\phi}{\theta_{\text{ap}}} \right)^2 \right] \left[\frac{1}{3} - \left(\frac{\phi}{\theta_{\text{ap}}} \right)^2 \right], \quad (3)$$

with the corresponding $Q(\phi)$,

$$Q(\phi) = \frac{6}{\pi\theta_{\text{ap}}^2} \left(\frac{\phi}{\theta_{\text{ap}}} \right)^2 \left[1 - \left(\frac{\phi}{\theta_{\text{ap}}} \right)^2 \right]. \quad (4)$$

A common definition of the “bias” parameter is the ratio of the variances of the galaxy and dark matter densities, which is the definition we will use here. In the case of deterministic, linear biasing, the galaxy density contrast δ_g is simply related to the mass density contrast δ as $\delta_g = b\delta$ (Kaiser 1987), and the ratio of the variances is the only relevant parameter. The galaxy number density contrast Δn_g is then

given by

$$\Delta n_g(\theta) = \frac{N(\theta) - \bar{N}}{\bar{N}} = b \int dw p_f(w) \delta[f_K(w)\theta; w], \quad (5)$$

where \bar{N} is the average number density of lens galaxies, w is the comoving distance, $f_K(w)$ is the comoving angular diameter distance, and where $p_f(w)dw$ corresponds to the redshift distribution of lens galaxies.

Then the aperture count, \mathcal{N} , is given by (Schneider 1998)

$$\mathcal{N}(\theta_{\text{ap}}) = \int d^2\phi U(\phi) \Delta n_g(\phi). \quad (6)$$

With our choice of the filter function $U(\phi)$, we can write the autocorrelation of \mathcal{N} as

$$\langle \mathcal{N}^2(\theta_{\text{ap}}) \rangle = 2\pi b^2 \int dw h_1(w; \theta_{\text{ap}}) \quad (7)$$

(Schneider 1998; van Waerbeke 1998; Hoekstra et al. 2001a), where $h_1(w; \theta_{\text{ap}})$ is defined as

$$h_1(w; \theta_{\text{ap}}) = \left[\frac{p_f(w)}{f_K(w)} \right]^2 P_{\text{filter}}(w; \theta_{\text{ap}}), \quad (8)$$

and where the “filtered” power spectrum $P_{\text{filter}}(w; \theta_{\text{ap}})$ is given by

$$P_{\text{filter}}(w; \theta_{\text{ap}}) = \int dl l P_{3d} \left[\frac{l}{f_K(w)}; w \right] J^2(l\theta_{\text{ap}}) \quad (9)$$

(Schneider et al. 1998).

Here P_{3d} is the time-evolving, three-dimensional power spectrum. As has been shown by Jain & Seljak (1997), it is important to use the nonlinear power spectrum in the calculations, and in the following, we use the results from Peacock & Dodds (1996). The filter function $J(\eta)$ is given by

$$J(\eta) = \frac{12}{\pi\eta^2} J_4(\theta), \quad (10)$$

where $J_4(x)$ is the fourth-order Bessel function of the first kind.

The power spectrum P_{3d} contains a wealth of information about the cosmological parameters. A measurement of $\langle \mathcal{N}^2 \rangle$ could be a powerful tool, provided the value of b is known. Unfortunately, the latter is not the case. This is why weak lensing by large-scale structure (“cosmic shear”) has become an important cosmological tool: it probes the (dark) matter power spectrum directly, without having to rely on the light distribution.

The matter autocorrelation function $\langle M_{\text{ap}} \rangle^2$ is related to the power spectrum as

$$\langle M_{\text{ap}}^2(\theta_{\text{ap}}) \rangle = \frac{9\pi}{2} \left(\frac{H_0}{c} \right)^4 \Omega_m^2 \int dw h_2(w; \theta_{\text{ap}}) \quad (11)$$

(Schneider et al. 1998), where Ω_m is the density parameter, and $h_2(w; \theta_{\text{ap}})$ is given by

$$h_2(w; \theta_{\text{ap}}) = \left[\frac{g(w)}{a(w)} \right]^2 P_{\text{filter}}(w; \theta_{\text{ap}}), \quad (12)$$

where $a(w)$ is the cosmic expansion factor. The function

$g(w)$ is given by

$$g(w) = \int_w^{w_H} dw' p_b(w') \frac{f_K(w' - w)}{f_K(w')} \quad (13)$$

and depends on the redshift distribution of the (background) sources $p_b(w)dw$. It measures the ‘‘lensing strength’’ of a lens at a distance w . If the lens is close to the sources, the lensing signal decreases, whereas a large distance between the lens and the sources results in a larger signal. Hence, $g(w)$ declines with increasing w , reaching a value of 1 for $w = 0$ and a value of 0 for lenses behind the sources.

We use equations (7) and (11) to relate the bias parameter b to the cosmology and measurements, and obtain

$$\begin{aligned} b^2 &= \frac{9}{4} \left(\frac{H_0}{c} \right)^2 \frac{\left[\int dw h_2(w; \theta_{\text{ap}}) \right]}{\left[\int dw h_1(w; \theta_{\text{ap}}) \right]} \Omega_m^2 \times \frac{\langle \mathcal{N}^2(\theta_{\text{ap}}) \rangle}{\langle M_{\text{ap}}^2(\theta_{\text{ap}}) \rangle} \\ &= f_1(\theta_{\text{ap}}, \Omega_m, \Omega_\Lambda) \times \Omega_m^2 \times \frac{\langle \mathcal{N}^2(\theta_{\text{ap}}) \rangle}{\langle M_{\text{ap}}^2(\theta_{\text{ap}}) \rangle}. \end{aligned} \quad (14)$$

The value of f_1 depends on the assumed cosmological model and the redshift distributions of the lenses and the sources. Hence, for a given cosmology, the bias parameter b can be determined from the observed ratio of the galaxy and matter autocorrelation functions. Calculations of f_1 as a function of aperture size show that it depends minimally on the aperture size and the adopted power spectrum.

The bias relation is likely to be more complicated than the simple case of linear deterministic biasing: the actual relation depends on the process of galaxy formation, and might be stochastic, nonlinear, or both. Hence, there is no reason that b is constant with scale, but as we demonstrate in the Appendix, we can still use equation (12) as long as b varies slowly with scale. Another complication is that b is likely to depend on redshift, and consequently, the derived value for b is a redshift-averaged value for the lenses in our sample.

If the bias parameter depends on redshift and scale, it is important that both the galaxy and matter autocorrelation functions probe the power spectrum at the same ‘‘effective’’ redshift. In addition, the interpretation is facilitated if the measurements probe a relatively small range in redshift. To examine this in more detail, it is useful to plot the $h_1(w; \theta_{\text{ap}})$ and $h_2(w; \theta_{\text{ap}})$ as a function of w .

The results are presented in Figure 1. The integrands have been normalized to a peak value of unity. The thick solid line shows $h_1(w; \theta_{\text{ap}})$ as a function of w for a fiducial $\theta_{\text{ap}} = 5'$. We used the observed redshift distribution of galaxies with $19.5 < R_C < 21$ from the CNOC2 survey, which gives rise to the wiggles in the function. This result indicates that we probe the power spectrum at an effective redshift ~ 0.35 . The thick dashed line shows $h_2(w; \theta_{\text{ap}})$ for the VIR-MOS-DESCART survey. This function is rather broad, which reflects the fact that weak lensing probes the power spectrum over a relatively large redshift range. However, comparison with the integrand for the galaxy autocorrelation function shows that both peak at the same redshift. Hence, we can use the ratio of $\langle \mathcal{N}^2 \rangle$ and $\langle M_{\text{ap}}^2 \rangle$ measured at the same aperture size θ_{ap} .

The lensing is maximal when the lens is halfway between the source and the observer. Hence, the weight function $h_2(w)$ reaches its peak value approximately halfway between the observer and the source. Compared to the

background galaxies from the VIR-MOS-DESCART survey, the RCS sources are at lower redshift, and consequently, the latter will probe the power spectrum at a lower redshift. This is indicated by the thin dashed line in Figure 1, which shows $h_2(w; \theta_{\text{ap}})$ using the RCS background galaxy redshift distribution. It is a poor match to the galaxy autocorrelation function. We therefore use the mass autocorrelation function measured from the VIR-MOS-DESCART survey.

So far, we have only used the autocorrelation functions. We can, however, also measure the galaxy-mass cross-correlation function $\langle \mathcal{N} M_{\text{ap}} \rangle$, which can be used to quantify how well the mass distribution correlates with the light distribution.

The galaxy-mass cross-correlation function $\langle \mathcal{N} M_{\text{ap}} \rangle$ is related to the power spectrum as

$$\langle M_{\text{ap}}(\theta_{\text{ap}}) \mathcal{N}(\theta_{\text{ap}}) \rangle = 3\pi \left(\frac{H_0}{c} \right)^2 \Omega_m b r \times \int dw h_3(w; \theta_{\text{ap}}) \quad (15)$$

(Schneider 1998; van Waerbeke 1998; Hoekstra et al. 2001a), where $h_3(w; \theta_{\text{ap}})$ is defined as

$$h_3(w; \theta_{\text{ap}}) = \frac{p_f(w)g(w)}{a(w)f_K(w)} P_{\text{filter}}(w; \theta_{\text{ap}}). \quad (16)$$

The parameter r in equation (15) is the galaxy-mass cross-correlation coefficient (Pen 1998; Dekel & Lahav 1999; Somerville et al. 2001), which is a measure of nonlinear stochastic biasing. In the case of deterministic linear biasing, $r = 1$.

The redshift distributions of the lenses and the sources used to measure the galaxy-mass cross-correlation function partly overlap. A source in front of a lens contributes no signal and therefore lowers the lensing signal. The overlap of the redshift distributions is naturally taken into account by equation (15). To prove this statement, we first consider a sheet of lenses at a distance ω_f . The ‘‘lensing strength’’ for these lenses is given by $g(\omega_f)$, to which only background galaxies with $\omega > \omega_f$ contribute. The larger the ω_f , the lower both the observed and predicted lensing signals will be (and they are lower by the same factor). Hence, equation (15) gives the correct result for a sheet of lenses at a given redshift. The actual redshift distribution of lenses can be considered a superposition of many sheets at different redshifts, and consequently, equation (15) is correct for any combination of lens and source redshift distributions.

The combination of equations (7), (11), and (15) relates the value of r to the observed correlation functions and the cosmology and is given by

$$\begin{aligned} r &= \frac{\sqrt{\int dw h_1(w; \theta_{\text{ap}})} \sqrt{\int dw h_2(w; \theta_{\text{ap}})}}{\int dw h_3(w; \theta_{\text{ap}})} \times \frac{\langle M_{\text{ap}} \mathcal{N} \rangle}{\langle M_{\text{ap}}^2 \rangle^{1/2} \langle \mathcal{N}^2 \rangle^{1/2}} \\ &= f_2(\theta_{\text{ap}}, \Omega_m, \Omega_\Lambda) \times \frac{\langle M_{\text{ap}}(\theta_{\text{ap}}) \mathcal{N}(\theta_{\text{ap}}) \rangle}{\sqrt{\langle \mathcal{N}^2(\theta_{\text{ap}}) \rangle} \langle M_{\text{ap}}^2(\theta_{\text{ap}}) \rangle}. \end{aligned} \quad (17)$$

Similar to f_1 , the value of f_2 depends minimally on θ_{ap} and the assumed power spectrum (van Waerbeke 1998).

The integrand $h_3(w; \theta_{\text{ap}})$ of the integral in equation (15) is also shown in Figure 1, and it matches the results for the galaxy autocorrelation function well. As for the bias parameter b , the value of r can depend on scale and redshift. However,

because of the properties of the aperture statistics described in the Appendix, we can measure the scale dependence of r directly from equation (17). As for b , the inferred value for r is a redshift-averaged value for the lenses in our sample.

Our definitions of b and r are chosen such that they can be related directly to the observed correlation functions. However, both b and the cross-correlation coefficient r mix nonlinear and stochastic effects (Dekel & Lahav 1999; Somerville et al. 2001), which we currently cannot disentangle with weak lensing.

Dekel & Lahav (1999) defined a combination of three parameters (\tilde{b} , \hat{b} , and σ_b) that separate nonlinear and stochastic biasing. They parametrize the stochasticity by the parameter σ_b , the local biasing scatter. The nonlinear biasing is characterized by the ratio \tilde{b}/\hat{b} , where \hat{b} is the slope of the linear regression of δ_g on δ (i.e., the natural generalization of the linear biasing parameter).

From lensing, we can only measure combinations of these parameters. We can, however, relate the observables b and r to the parameters from Dekel & Lahav (1999) in the two limiting cases. If we assume that the bias is purely nonlinear and deterministic (i.e., $\sigma_b = 0$), we obtain $\tilde{b} = b$ and $\tilde{b}/\hat{b} = 1/r$. Hence, the inverse of the cross-correlation coefficient measures the amount of nonlinear biasing. Likewise, in the case of linear and stochastic biasing (i.e., $\tilde{b} = \hat{b}$), we obtain $\sigma_b = b(1 - r^2)^{1/2}$.

4. DETERMINATION OF THE CORRELATION FUNCTIONS

A straightforward implementation of the method described above is to tile the survey area with apertures and compute $\langle M_{\text{ap}, \mathcal{N}} \rangle(\theta)$ and $\langle \mathcal{N}^2 \rangle(\theta)$ directly from the data. To do so, one can use the estimators (Schneider 1998)

$$\tilde{M}_{\text{ap}} = \pi \theta_{\text{ap}}^2 \frac{\sum_{i=1}^{N_b} Q(\theta_i) w_i \gamma_{t,i}}{\sum_{i=1}^{N_b} w_i}, \quad \tilde{\mathcal{N}} = \frac{1}{N} \sum_{i=1}^{N_f} U(\theta_i),$$

where N_f and N_b are the number of lens and source galaxies, respectively, found in the aperture of radius θ_{ap} , N is the average number density of lenses, and $\gamma_{t,i}$ is the observed tangential shear of the i th background galaxy. The weights w_i correspond to the inverse square of the uncertainty in the shear measurement (Hoekstra et al. 2000).

However, this procedure has the disadvantage that it assumes a contiguous data set; i.e., there are no holes in the data. In real data, regions that are contaminated by bright stars, bad columns, etc., have to be masked. Although the masking of the RCS data is not severe, we will use a different approach, which is much less sensitive to the geometry of the survey.

We measure instead the ensemble-averaged tangential shear as a function of radius around the sample of lenses (“galaxy-galaxy lensing” signal) and use these results to derive $\langle M_{\text{ap}, \mathcal{N}} \rangle$. We use the angular two-point correlation function to estimate $\langle \mathcal{N}^2 \rangle$. The mass autocorrelation function $\langle M_{\text{ap}}^2 \rangle$ is derived from the observed ellipticity correlation functions (Pen et al. 2002; van Waerbeke et al. 2002; Hoekstra et al. 2002b). We show below how these observed correlation functions, which do not require contiguous survey areas, can be easily related to the aperture mass correlation functions.

We first consider the angular two-point correlation function $\omega(\theta)$, which is related to the power spectrum through

$$\omega(\theta) = \langle \Delta n_g(0) \Delta n_g(\theta) \rangle = \frac{b^2}{2\pi} \int dw \left[\frac{p_f(w)}{f_K(w)} \right]^2 \times \int dl l P_{3d} \left[\frac{l}{f_K(w)}; w \right] J_0(l\theta), \quad (18)$$

where $J_0(x)$ is the zeroth-order Bessel function of the first kind. We can define the effective (projected) power spectrum of the angular correlation function $P_\omega(l)$ as

$$P_\omega(l) = b^2 \int dw \left[\frac{p_f(w)}{f_K(w)} \right]^2 P_{3d} \left[\frac{l}{f_K(w)}; w \right]. \quad (19)$$

Thus, we obtain for the angular correlation function

$$\omega(\theta) = \frac{1}{2\pi} \int dl l P_\omega(l) J_0(l\theta). \quad (20)$$

For the autocorrelation function of \mathcal{N} , we have (see eqs. [7] and [9])

$$\langle \mathcal{N}^2 \rangle(\theta) = 2\pi \int dl l P_\omega(l) \left[\frac{12J_4(l\theta)}{\pi(l\theta)^2} \right]^2. \quad (21)$$

Schneider, van Waerbeke, & Mellier (2002) have shown that it is rather straightforward to transform one correlation function into another. Using the orthogonality of Bessel functions, we obtain

$$P_\omega(l) = 2\pi \int d\vartheta \vartheta \omega(\vartheta) J_0(l\vartheta), \quad (22)$$

which we can use to relate $\langle \mathcal{N}^2 \rangle(\theta)$ to $\omega(\theta)$. Doing so, we obtain

$$\langle \mathcal{N}^2 \rangle(\theta) = \int d\vartheta \frac{\vartheta}{\theta^2} \omega(\vartheta) T_+ \left(\frac{\vartheta}{\theta} \right), \quad (23)$$

where the function $T_+(x)$ is defined as (Schneider et al. 2002)

$$T_+(x) = 576 \int_0^\infty \frac{dt}{t^3} J_0(xt) [J_4(t)]^2. \quad (24)$$

Schneider et al. (2002) found an expression for $T_+(x)$ in terms of elementary functions,

$$T_+(x) = \frac{6(2 - 15x^2)}{5} \left[1 - \frac{2}{\pi} \arcsin(x/2) \right] + \frac{x\sqrt{4 - x^2}}{100\pi} (120 + 2320x^2 - 754x^4 + 132x^6 - 9x^8), \quad (25)$$

for $x \leq 2$. $T_+(x)$ vanishes for $x > 2$. Therefore, the integral in equation (19) extends only over $0 \leq \vartheta \leq 2\theta$. Hence, we need to measure the angular correlation function out to twice the aperture size in order to compute $\langle \mathcal{N}^2 \rangle(\theta)$.

We now turn to the measurement of the galaxy-mass cross-correlation function. In this case, the azimuthally averaged tangential shear around the lens galaxies is a very useful statistic (e.g., Fischer et al. 2000). To derive the galaxy-mass correlation function, we use the relation between the average convergence $\bar{\kappa}(\theta)$ inside a circular aperture of

radius θ and the mean tangential shear along the boundary of the aperture

$$\langle \gamma_t \rangle(\theta) = -\frac{1}{2} \frac{d\bar{\kappa}(\theta)}{d \ln \theta}. \quad (26)$$

The galaxy-mass correlation function is defined as $\langle \Delta n_g(0) \gamma_t(\theta) \rangle = \langle \gamma_t \rangle(\theta)$ and is related to the power spectrum as

$$\langle \gamma_t \rangle(\theta) = \frac{3\Omega_m}{4\pi} \left(\frac{H_0}{c} \right)^2 br \int dw \frac{g(w)p_f(w)}{a(w)f_K(w)} \times \int dl l P_{3d} \left[\frac{l}{f_K(w)}; w \right] J_2(l\theta) \quad (27)$$

(Kaiser 1992; Guzik & Seljak 2001), where $J_2(x)$ is the second-order Bessel function of the first kind. We assume that the cross power spectrum is related to the matter power spectrum by $brP_{3d}(k)$. As discussed above, the assumption of a constant value of b and r does not change the interpretation of our measurements.

We define the effective (projected) power spectrum for the galaxy-mass correlation function $P_\gamma(l)$ as

$$P_\gamma(l) = \frac{3}{2} \left(\frac{H_0}{c} \right)^2 \Omega_m br \times \int dw \frac{g(w)p_f(w)}{a(w)f_K(w)} P_{3d} \left[\frac{l}{f_K(w)}; w \right], \quad (28)$$

which gives

$$\langle \gamma_t \rangle(\theta) = \frac{1}{2\pi} \int dl l P_\gamma(l) J_2(l\theta) \quad (29)$$

and

$$\langle \mathcal{N} M_{\text{ap}} \rangle(\theta) = 2\pi \int dl l P_\gamma(l) \left[\frac{12J_4(l\theta)}{\pi(l\theta)^2} \right]^2. \quad (30)$$

As before, we can express $P_\gamma(l)$ by an integral over the galaxy-mass cross-correlation function, and we obtain

$$\langle \mathcal{N} M_{\text{ap}} \rangle(\theta) = \int d\vartheta \frac{\vartheta}{\theta^2} \langle \gamma_t \rangle(\vartheta) F \left(\frac{\vartheta}{\theta} \right), \quad (31)$$

where we define the function $F(x)$ as

$$F(x) = 576 \int_0^\infty \frac{dt}{t^3} J_2(xt) [J_4(t)]^2. \quad (32)$$

We did not find a simple expression for this function, but it is well-behaved for $0 \leq x \leq 2$ and vanishes for $x > 2$. Hence, as before, the integral in equation (31) extends over only $0 \leq \vartheta \leq 2\theta$.

The mass autocorrelation function $\langle M_{\text{ap}}^2 \rangle$ can be obtained by measuring the ellipticity correlation functions, which are given by

$$\xi_{tt}(\theta) = \frac{\sum_{i,j}^{N_s} w_i w_j \gamma_{t,i}(\mathbf{x}_i) \cdot \gamma_{t,j}(\mathbf{x}_j)}{\sum_{i,j}^{N_b} w_i w_j}, \quad (33)$$

$$\xi_{rr}(\theta) = \frac{\sum_{i,j}^{N_s} w_i w_j \gamma_{r,i}(\mathbf{x}_i) \cdot \gamma_{r,j}(\mathbf{x}_j)}{\sum_{i,j}^{N_b} w_i w_j}, \quad (34)$$

where $\theta = |\mathbf{x}_i - \mathbf{x}_j|$; γ_t and γ_r are the tangential and 45°

rotated shear in the frame defined by the line connecting the pair of galaxies. For the following, it is more useful to consider

$$\xi_+(\theta) = \xi_{tt}(\theta) + \xi_{rr}(\theta), \quad \xi_-(\theta) = \xi_{tt}(\theta) - \xi_{rr}(\theta), \quad (35)$$

i.e., the sum and the difference of the two observed correlation functions. As shown by Crittenden et al. (2002), one can derive E - and B -mode correlation functions by integrating $\xi_+(\theta)$ and $\xi_-(\theta)$ with an appropriate window function (see Pen et al. 2002 for an application to the VIRMOS-DESCART data).

The E - and B -mode aperture masses are computed from the ellipticity correlation functions using (Crittenden et al. 2002; Schneider et al. 2002)

$$\langle M_{\text{ap}}^2 \rangle(\theta) = \frac{1}{2} \int \frac{d\vartheta}{\theta_{\text{ap}}^2} \vartheta \left[\xi_+(\vartheta) T_+ \left(\frac{\vartheta}{\theta_{\text{ap}}} \right) + \xi_-(\vartheta) T_- \left(\frac{\vartheta}{\theta_{\text{ap}}} \right) \right] \quad (36)$$

and

$$\langle M_{\perp}^2 \rangle(\theta) = \frac{1}{2} \int \frac{d\vartheta}{\theta_{\text{ap}}^2} \vartheta \left[\xi_+(\vartheta) T_+ \left(\frac{\vartheta}{\theta_{\text{ap}}} \right) - \xi_-(\vartheta) T_- \left(\frac{\vartheta}{\theta_{\text{ap}}} \right) \right]. \quad (37)$$

The expression for $T_+(x)$ is given by equation (22), whereas $T_-(x)$ is given by

$$T_-(x) = \frac{192}{35\pi} x^3 \left(1 - \frac{x^2}{4} \right)^{7/2} \quad (38)$$

for $x \leq 2$ and $T_-(x)$ vanishes for $x > 2$.

The B -mode aperture mass $\langle M_{\perp}^2 \rangle$ provides a quantitative estimate of the systematics, since gravitational lensing only produces an E mode. Residual systematics (e.g., imperfect correction for the point-spread function anisotropy) or intrinsic alignments will give rise to a B mode. A similar test exists for the galaxy-mass cross-correlation function: in the absence of systematics, the average signal around the lenses should vanish when the sources are rotated by 45° .

5. MEASUREMENTS

In this section, we present the measurements of the galaxy autocorrelation and the galaxy-mass cross-correlation function $\langle M_{\text{ap}}(\theta_{\text{ap}}) \mathcal{N}(\theta_{\text{ap}}) \rangle$, which were obtained from the RCS data. The mass autocorrelation function $\langle M_{\text{ap}}^2(\theta_{\text{ap}}) \rangle$ was measured by van Waerbeke et al. (2002) from the VIRMOS-DESCART survey.

As described in §4, we do not measure $\langle \mathcal{N}^2 \rangle$ directly from the data. Instead, we measure the angular correlation function $\omega(\theta)$ and use equation (23) to determine $\langle \mathcal{N}^2 \rangle$. To measure $\omega(\theta)$, we use the well-known estimator (Landy & Szalay 1993)

$$\omega(\theta) = \frac{DD - 2DR + RR}{RR}, \quad (39)$$

where DD , DR , and RR are pair counts in bins of $\theta + \delta\theta$ of the data-data, data-random, and random-random points, respectively. For each patch, we create 24 mock catalogs by placing the lens galaxies at random positions in the unmasked regions of the data. We note our sample of lenses is complete within the unmasked regions: the galaxies are

sufficiently faint that they are not saturated, and they are several magnitudes brighter than the detection limit. Furthermore, the uncertainties in the photometry are small (less than 3%; M. D. Gladders et al. 2002, in preparation) and do not affect the measurement of the angular correlation function of the lens galaxies.

In order to determine the true angular correlation function, one needs to apply an integral constraint correction to the observed correlation function. The determination of this correction is not trivial and can introduce a significant systematic uncertainty. However, since the integral $\int dx x T_+(x)$ vanishes, $\langle \mathcal{N}^2 \rangle$ has the nice property of being independent of the integral constraint correction. In addition, the measurements on different scales are only mildly correlated.

Although we use the observed angular correlation function as an intermediate step in our analysis, it is useful to compare the results to previous work. The observed angular correlation function is well-approximated by a power law with slope -0.7 and an amplitude $\omega(1') = 0.115 \pm 0.005$. Unfortunately, a direct comparison with the literature is difficult because of the different sample selection (magnitude limits, filters). We can, however, make a crude comparison with the results from Postman et al. (1998), who measured the angular correlation function in the I band. The mean R_C -band magnitude of our sample is ~ 20.5 , which corresponds to a mean I -band magnitude of ~ 19.8 (based on the colors of galaxies observed in the CNOC2 survey). Postman et al. (1998) list a value of $\omega(1') = 0.136 \pm 0.021$ for galaxies with a median magnitude of $I = 19.6$, which is in reasonable agreement with our result.

We measured $\langle \mathcal{N}^2 \rangle$ for each of the 10 RCS patches and used the scatter in these measurements to estimate the error bars on the galaxy autocorrelation function. The errors, therefore, also include cosmic variance. The results, measured out to 1° , are presented in Figure 2a.

Figure 2b shows the cross-correlation function $\langle M_{\text{ap}} \mathcal{N} \rangle$ as measured from the RCS. To derive the cross-correlation function, we measured the azimuthally averaged tangential shear around the lens galaxies in bins of $1''$. We then used equation (31) to relate the observed tangential shear profile to $\langle M_{\text{ap}} \mathcal{N} \rangle$. As before, we measured the cross-correlation for the 10 RCS patches and used the scatter in the measurements to estimate the error bars.

The mass autocorrelation function $\langle M_{\text{ap}}^2 \rangle$ presented in Figure 2c was taken from van Waerbeke et al. (2002). It was derived from the observed ellipticity correlation functions (see eq. [36]). The largest scale measurement of $\langle M_{\text{ap}}^2 \rangle$ from the VIRMO-DESCART survey is $45'$. The error bars in Figure 2c have been increased to account for the unknown correction for the observed B mode (van Waerbeke et al. 2002).

The shapes and amplitudes of the correlation functions presented in Figure 2 depend on the power spectrum. As discussed in § 3, we can remove the dependence on the power spectrum by taking ratios of the correlation functions. Since the various correlation functions probe the power spectrum at the same redshift (see Fig. 1), we can take the ratios of measurements at the same angular scale. If the surveys were not well matched, we would have had to compare the measurements at different angular scales in order to ensure that we probe the power spectrum at the same physical scale. In addition, one has to take into account the evolution of the power spectrum in such a situation.

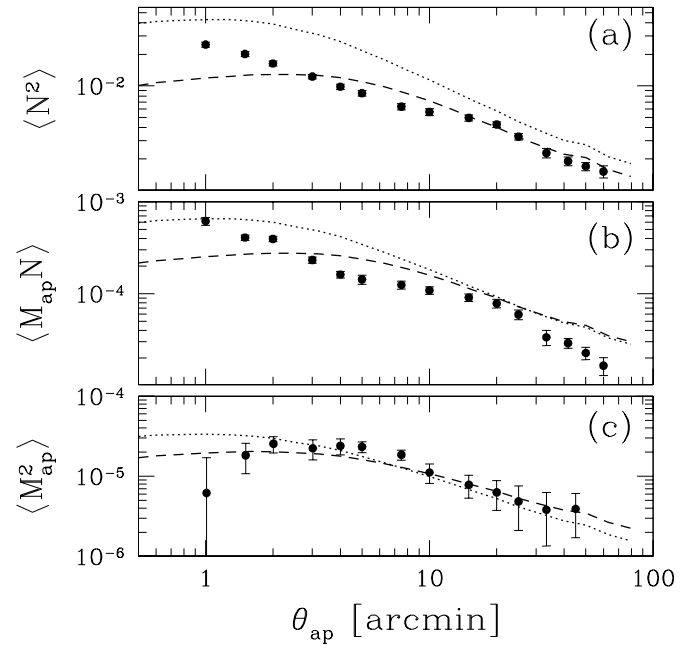


FIG. 2.— Measurements of (a) $\langle \mathcal{N}^2 \rangle$ and (b) $\langle \mathcal{N} M_{\text{ap}} \rangle$ as a function of angular scale from the RCS data. The largest scale corresponds to an aperture radius of 1° . (c) $\langle M_{\text{ap}}^2 \rangle$ as a function of angular scale from the VIRMO-DESCART data (largest scale is $45'$). The error bars for $\langle M_{\text{ap}}^2 \rangle$ have been increased to account for the unknown correction for the observed B mode. For reference (they are not fitted to the measurements), we have also plotted model predictions (for $b = 1$ and $r = 1$) for an OCDM cosmology (dotted line: $\Omega_m = 0.3$, $\Omega_\Lambda = 0$, $\sigma_8 = 0.9$, and $\Gamma = 0.21$) and a Λ CDM cosmology (dashed line: $\Omega_m = 0.3$, $\Omega_\Lambda = 0.7$, $\sigma_8 = 0.9$, and $\Gamma = 0.21$). Note that the points at different scales are slightly correlated.

The observed ratio $\langle M_{\text{ap}} \mathcal{N} \rangle / (\langle \mathcal{N}^2 \rangle \langle M_{\text{ap}}^2 \rangle)^{1/2}$ as a function of aperture size is presented in Figure 3a. Figure 3b gives the ratio of $\langle M_{\text{ap}}^2 \rangle$ and $\langle \mathcal{N}^2 \rangle$. The error bars on the ratios correspond to the 68% confidence limits and have been determined from a Monte Carlo simulation using the uncertainties in the measurements of the observed correlation functions (which were assumed to be Gaussian). For reference, we have also indicated the effective physical scale (\sim FWHM of the filter function) probed by the compensated filter $U(\phi)$, corresponding to a redshift of $z = 0.35$.

For reference, Figure 3 also shows the ratios for an OCDM and a Λ CDM model in the case $b = 1$ and $r = 1$ (i.e., we have plotted $\Omega_m^2 \times f_1$, and f_2). These model values are virtually constant with scale if b and r are constant. Also note that the value for the cross-correlation is almost the same for both cosmologies, whereas the ratio of the autocorrelation functions differs by almost a factor of 2.

To examine possible systematic effects, we also computed the results when the sources are rotated by 45° . This signal should vanish in the case of lensing. The results of this powerful test for the cross-correlation are presented in Figure 4 and are indeed consistent with no signal. The results for the autocorrelation do show some residual systematics. The amplitude of this signal is added to the error estimates in Figure 3b as a conservative limit (van Waerbeke et al. 2002). We note that the amplitude of the B -mode signal is small compared to the lensing (E -mode) signal. Based on these results, we conclude that the accuracy of our measurements (in particular, the galaxy-mass cross-correlation) is not limited by systematics.

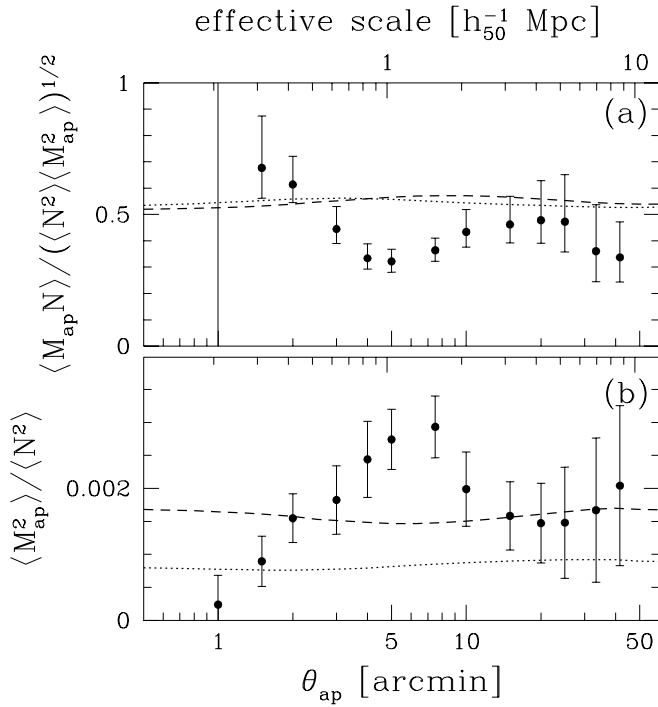


FIG. 3.—(a) Observed ratio $\langle M_{\text{ap}} \mathcal{N} \rangle / (\langle \mathcal{N}^2 \rangle \langle M_{\text{ap}}^2 \rangle)^{1/2}$ as a function of aperture size. (b) Ratio of the mass autocorrelation $\langle M_{\text{ap}}^2 \rangle$ and the galaxy autocorrelation $\langle \mathcal{N}^2 \rangle$ as a function of aperture size. The measurements at different scale are slightly correlated, and the error bars correspond to the 68% confidence intervals. *Upper axis*: Effective physical scale probed by the compensated filter $U(\phi)$ at the median redshift of the lenses ($z = 0.35$). *Dotted lines*: Predictions of an OCDM model, whereas the dashed lines correspond to the Λ CDM model for $b = 1$, and $r = 1$. In both cases, if b , and r are constant with scale, we expect to observe ratios that are virtually constant. The observed ratios show significant variation with scale, thus implying that both b and r vary.

6. DISCUSSION

The results presented in Figure 3 suggest significant variation of both b and r with scale. We convert the observed ratios into estimates for the bias parameters for the currently favored cosmological model ($\Omega_m = 0.3$, $\Omega_\Lambda = 0.7$) using equations (14) and (17).

Figure 5a shows the inferred value of the galaxy-mass cross-correlation coefficient r as a function of scale. Because of the small value of $\langle M_{\text{ap}}^2 \rangle$ at $1'$, the uncertainties in both b and r are very large, and we have omitted this point.

We find that on small scales, the measurements are consistent with a value $r \sim 1$. This good correlation between mass and light on small scales (i.e., around galaxies) indicates that (luminous) galaxies are surrounded by massive halos. We note that with our definition, r can be larger than 1. On the largest scales, the results are consistent with $r = 1$. On scales $\sim 1 h_{50}^{-1}$ Mpc, r is significantly lower than unity, with a minimum value of $r = 0.57^{+0.08}_{-0.07}$ (68% confidence).

Figure 5b shows that the scale dependence of b is very similar to that of r (also see Fig. 6). We find that b is smaller than unity on scales $\sim 1-2 h_{50}^{-1}$ Mpc, with a minimum value of $b = 0.71^{+0.06}_{-0.05}$ (at $1.5 h_{50}^{-1}$ Mpc; 68% confidence). Hence, the dark matter is more strongly clustered than the galaxies. The variation of b with scale is significant, but a better determination of $\langle M_{\text{ap}}^2 \rangle$ is needed to study the scale dependence in more detail.

Our result is in good qualitative agreement with the findings of Jenkins et al. (1998), who combined the observed

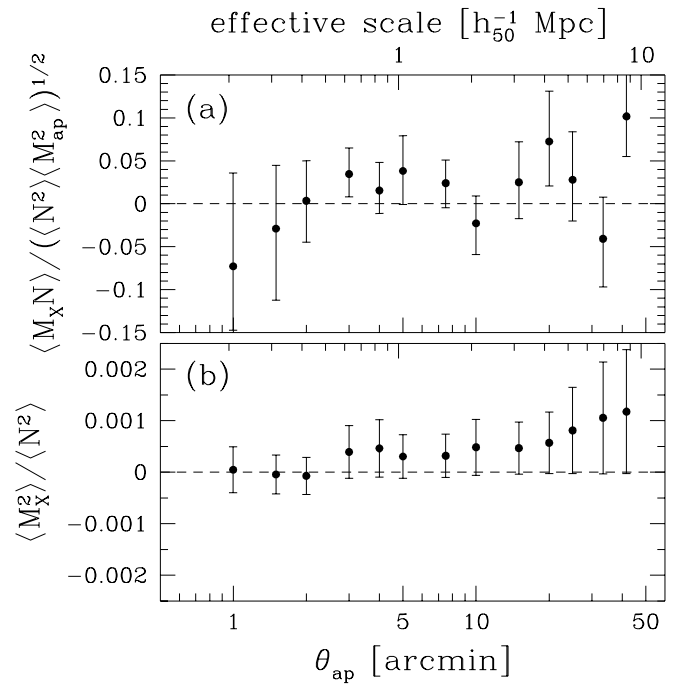


FIG. 4.—(a) Observed ratio $\langle M_X \mathcal{N} \rangle / (\langle \mathcal{N}^2 \rangle \langle M_{\text{ap}}^2 \rangle)^{1/2}$ as a function of aperture size. This corresponds to the results when the phase of the shear is increased by $\pi/2$. If the signal presented in Figure 3a is caused by lensing, it should vanish here, as it does. (b) Ratio of the B mode autocorrelation $\langle M_X^2 \rangle$ and the galaxy autocorrelation $\langle \mathcal{N}^2 \rangle$ as a function of aperture size. The results suggest a residual B mode, which is attributed to systematics (note that the points at different scales are somewhat correlated). The amplitude of this signal is added to the error estimates in Figure 3b as a conservative limit. We note that the amplitude of the B mode signal is small compared to the lensing (E mode) signal.

Automated Plate Measuring Facility (APM) two-point correlation function and the matter correlation function derived from numerical simulations. We note that a direct comparison cannot be made with other measurements (such as those from Jenkins et al. 1998), because the bias properties depend on galaxy type and redshift. For instance, observations show that the amplitude of the galaxy correlation function depends on luminosity (Benoist et al. 1996; Norberg et al. 2001).

Our results are derived for a specific subset of galaxies and are redshift-averaged values (the lenses have a large range in redshift, with intrinsically brighter galaxies at higher redshifts). This is clearly demonstrated by equation (A7). In the simple case in which the average bias parameters change approximately linearly with redshift, our results can be interpreted as a measurement of the biasing properties of L_* galaxies at redshift ~ 0.35 . However, the redshift dependence of the bias in magnitude-limited samples is usually more complex.

Hoekstra et al. (2001a) measured the ratio b/r on angular scales out to $12.5'$ and found that the results were consistent with a constant value. With the additional data (which probe larger scales and give smaller error bars), we find evidence for a small trend with scale. The measurements of the current RCS data extend out to an angular scale of 1° (which corresponds to a physical scale of $12.5 h_{50}^{-1}$ Mpc) and are presented in Figure 6a. Figure 6 shows that even on a 1° scale, the systematics are much smaller than the signal. Hence, the value of b/r can be determined accurately. The

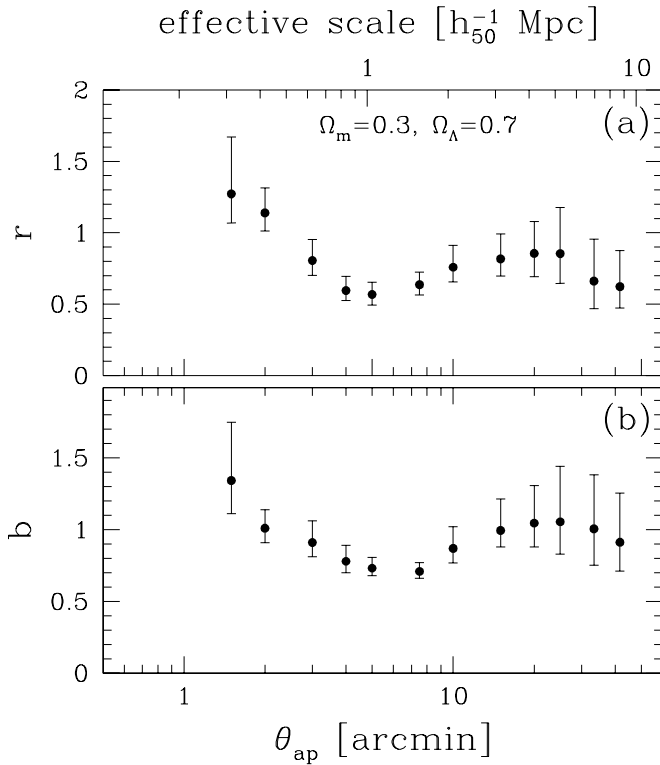


FIG. 5.—(a) Measured value of the galaxy-mass cross correlation coefficient r as a function of scale for the Λ CDM cosmology. (b) Bias parameter b as a function of scale. Upper axis: Effective physical scale probed by the compensated filter $U(\phi)$ at the median redshift of the lenses ($z = 0.35$). The error bars correspond to the 68% confidence intervals. Note that the measurements at different scales are slightly correlated.

new data yield an average value of $b/r = 1.090 \pm 0.035$. Limiting the measurements to the angular scales studied in Hoekstra et al. (2001a), we find an average value of $b/r = 1.05 \pm 0.04$, in excellent agreement with the previous estimate of $b/r = 1.05^{+0.12}_{-0.10}$.

Our measurements should be compared to models of galaxy formation. The two commonly used approaches are hydrodynamic simulations (e.g., Blanton et al. 2000; Yoshikawa et al. 2001) or semianalytical models (e.g., Kauffmann et al. 1999a, 1999b; Somerville et al. 2001; Guzik & Seljak 2001). These studies suggest values of r close to unity. Unfortunately, the mass resolution in these simulations, such as the GIF results (Kauffmann et al. 1999a, 1999b) is too poor: they only resolve massive, luminous galaxies. Our sample of lenses contains many lower-luminosity systems, which seriously hampers the comparison of our results with predictions.

As the value of r is intimately linked to the details of galaxy formation, a careful comparison of the models with the weak lensing measurements provides unique constraints. In

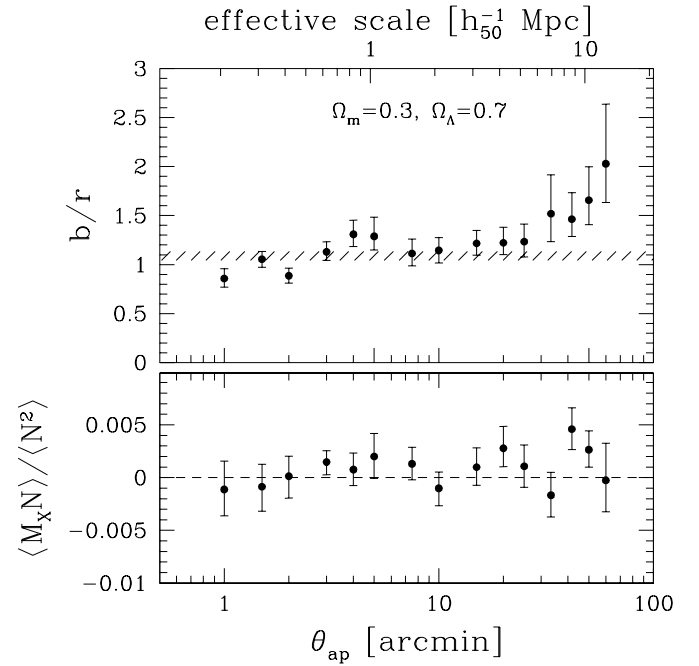


FIG. 6.—(a) Value of b/r as a function of angular scale under the assumption $\Omega_m = 0.3$ and $\Omega_\Lambda = 0.7$. These results are based on RCS data only, which allows this ratio to measured out to 1° (which corresponds to a physical scale of $12.5 h_{50}^{-1}$ Mpc). Note that the points are slightly correlated. The value of b/r is almost constant over the range probed here. For this cosmology, we find an average value of $b/r = 1.090 \pm 0.035$, in excellent agreement with the result from Hoekstra et al. (2001a). (b) Measurement of $\langle M_X N \rangle / \langle N^2 \rangle$ (the signal when the phase of the shear is increased by $\pi/2$), which should vanish if the results in (a) are caused by lensing.

addition, planned large weak lensing surveys such as the CFHT Legacy Survey⁹ will significantly improve the accuracy of the measurements, allowing larger scales to be probed and enabling us to select galaxies based on colors or luminosities (using photometric redshifts). Therefore, the prospects of constraining biasing parameters from weak lensing are excellent.

We thank the anonymous referee for his comments, which helped to improve the paper significantly. The RCS is supported by a NSERC operating grant to H. Y. We thank the VIRMOS and Terapix teams who obtained and processed the VIRMOS-DESCART data. This VIRMOS-DESCART survey was supported by the TMR Network “Gravitational Lensing: New Constraints on Cosmology and the Distribution of Dark Matter” of the EC under contract ERBFMRX-CT97-0172. Y. M. thanks CITA for hospitality. It is a pleasure to thank Simon White, Peter Schneider, and Francis Bernardeau for useful discussions.

⁹ Go to <http://www.cfht.hawaii.edu/Science/CFHLS/>.

APPENDIX

SCALE AND REDSHIFT-DEPENDENT BIAS PARAMETERS

As has been demonstrated in this paper, the bias relation is more complicated than the simple case of linear deterministic biasing, and the inferred values of b and r vary with scale. In addition, these parameters are expected to vary with redshift.

In § 3, we treated both b and r as constants, which is not warranted by the data. In this appendix, however, we show that as long as b and r vary slowly with scale, we can still infer the bias parameters as a function of scale directly. This procedure works because the aperture mass statistic is effectively a passband filter.

If we assume that $\delta_g(k) = b(k)\delta(k)$, we have to replace equation (5) with

$$\Delta n_g(\theta) = \int dw p_f(w) b[f_K(w)\theta; w] \delta[f_K(w)\theta; w], \quad (\text{A1})$$

which changes the galaxy autocorrelation function to

$$\langle \mathcal{N}^2(\theta_{\text{ap}}) \rangle = 2\pi \int dw \frac{p_f^2(w)}{f_K^2(w)} \tilde{P}_{\text{filter}}(w; \theta_{\text{ap}}), \quad (\text{A2})$$

where

$$\tilde{P}_{\text{filter}}(w; \theta_{\text{ap}}) = \int dl l b^2 \left[\frac{l}{f_K(w)}; w \right] P_{3d} \left[\frac{l}{f_K(w)}; w \right] J^2(l\theta_{\text{ap}}). \quad (\text{A3})$$

The filter $J^2(\eta)$ is strongly peaked, and this motivates the approximation of J^2 by a Dirac delta function (Bartelmann & Schneider 1999),

$$J^2(\eta) \approx \frac{512}{1155\pi^3} \delta(\eta - 693\pi/512) \approx 1.43 \times 10^{-2} \delta(\eta - 4.25). \quad (\text{A4})$$

Consequently, $\tilde{P}_{\text{filter}}$ can be approximated as

$$\tilde{P}_{\text{filter}}(w; \theta_{\text{ap}}) \approx b^2 \left[\frac{4.25}{\theta_{\text{ap}} f_K(w)}; w \right] P_{\text{filter}}(w; \theta_{\text{ap}}), \quad (\text{A5})$$

where P_{filter} is given by equation (9). For the ratio of the galaxy and matter autocorrelation functions, we can write

$$\frac{\langle M_{\text{ap}}^2 \rangle}{\langle \mathcal{N}^2 \rangle} \approx \frac{9}{4} \left(\frac{H_0}{c} \right)^4 \Omega_m^2 \frac{\int dw h_2(w; \theta_{\text{ap}})}{\int dw h_1(w; \theta_{\text{ap}}) b^2 \{4.25/[\theta_{\text{ap}} f_K(w)]; w\}} \quad (\text{A6})$$

or

$$\frac{\int dw h_1(w; \theta_{\text{ap}}) b^2 \{4.25/[\theta_{\text{ap}} f_K(w)]; w\}}{\int dw h_1(w; \theta_{\text{ap}})} = \frac{9}{4} \left(\frac{H_0}{c} \right)^4 \Omega_m^2 \frac{\int dw h_2(w; \theta_{\text{ap}}) \langle \mathcal{N}^2 \rangle}{\int dw h_1(w; \theta_{\text{ap}}) \langle M_{\text{ap}}^2 \rangle} = f_1 \times \Omega_m^2 \times \frac{\langle \mathcal{N}^2 \rangle}{\langle M_{\text{ap}}^2 \rangle}(\theta_{\text{ap}}). \quad (\text{A7})$$

The functions h_1 , and h_2 are given by equations (8) and (12). The actual calculations show that f_1 does not depend on the power spectrum (van Waerbeke 1998). The left-hand side of equation (A7) shows that we measure the bias parameter weighted by the function h_1 .

A similar result can be obtained for the galaxy-mass cross-correlation coefficient r ,

$$\frac{\int dw h_3(w; \theta_{\text{ap}}) r \{4.25/[\theta_{\text{ap}} f_K(w)]; w\}}{\int dw h_3(w; \theta_{\text{ap}})} = \frac{\sqrt{\int dw h_1(w; \theta_{\text{ap}})} \sqrt{\int dw h_2(w; \theta_{\text{ap}})}}{\int dw h_3(w; \theta_{\text{ap}})} \times \frac{\langle M_{\text{ap}} \mathcal{N} \rangle}{\sqrt{\langle \mathcal{N}^2 \rangle \langle M_{\text{ap}}^2 \rangle}} = f_2 \times \frac{\langle M_{\text{ap}}(\theta_{\text{ap}}) \mathcal{N}(\theta_{\text{ap}}) \rangle}{\sqrt{\langle \mathcal{N}^2(\theta_{\text{ap}}) \rangle \langle M_{\text{ap}}^2(\theta_{\text{ap}}) \rangle}}. \quad (\text{A8})$$

The redshift distribution of the lenses $p_f(w)$ is narrow (see Fig. 1). Hence, we measure the bias parameters over a small range in redshift. Because $f_K(w)$ varies somewhat over this interval, we average values of b and r on different physical scales. However, if b and r vary slowly with scale and redshift, we can ignore the variation of these parameters over this range in scale. Hence, equations (12) and (14) can be used to obtain direct measurements of the bias parameters as a function of scale.

REFERENCES

- Bacon, D., Massey, R., Refregier, A., & Ellis, R. 2002, MNRAS, submitted (astro-ph/0203134)
- Bartelmann, M., & Schneider, P. 1999, A&A, 345, 17
- Benoist, C., Maurogordato, S., da Costa, L. N., Cappi, A., & Schaeffer, R. 1996, ApJ, 472, 452
- Blanton, M. 2000, ApJ, 544, 63
- Blanton, M., Cen, R., Ostriker, J. P., Strauss, M. A., & Tegmark, M. 2000, ApJ, 531, 1
- Crittenden, R. G., Natarajan, P., Pen, U.-L., & Theuns, T. 2002, ApJ, 568, 20
- Dekel, A., & Lahav, O. 1999, ApJ, 520, 24
- Fernández-Soto, A., Lanzetta, K. M., & Yahil, A. 1999, ApJ, 513, 34
- Fischer, P., et al. 2000, AJ, 120, 1198
- Guzik, J., & Seljak, U. 2001, MNRAS, 321, 439
- Hoekstra, H., Franx, M., & Kuijken, K. 2000, ApJ, 532, 88
- Hoekstra, H., Yee, H. K. C., & Gladders, M. D. 2001a, ApJ, 558, L11
- . 2001b, Where's the Matter? Tracing Dark and Bright Matter with the New Generation of Large-Scale Surveys, ed. Treyer & Tresse (astro-ph/0109514)
- . 2002b, ApJ, 577, in press
- Hoekstra, H., Yee, H. K. C., Gladders, M. D., Barrientos, L. F., Hall, P. B., & Infante, L. 2002a, ApJ, 572, 55
- Jain, B., & Seljak, U. 1997, ApJ, 484, 560
- Jenkins, A., et al. 1998, ApJ, 499, 20
- Kaiser, N. 1992, ApJ, 388, 272
- . 1987, MNRAS, 227, 1
- Kaiser, N., Squires, G., Fahlman, G. G., & Woods, D. 1994, Clusters of Galaxies, ed. Durret, Mazure, & Tran Thanh Van, 269
- Kauffmann, G., Colberg, J. M., Diaferio, A., & White, S. D. M. 1999a, MNRAS, 303, 188
- . 1999b, MNRAS, 307, 529
- Landy, S. D., & Szalay, A. S. 1993, ApJ, 12, 64
- McKay, T. A., et al. 2001, ApJ, submitted (astro-ph/0108013)
- Norberg, P., et al. 2002, MNRAS, 332, 827
- Peacock, J. A., & Dodds, S. J. 1996, MNRAS, 280, L19
- Peacock, J. A., et al. 2001, Nature, 410, 169
- Pen, U.-L. 1998, ApJ, 504, 601
- Pen, U.-L., van Waerbeke, L., & Mellier, Y. 2002, ApJ, 567, 31
- Postman, M., Laver, T. R., Szapudi, I., & Oegerle, W. 1998, ApJ, 506, 33
- Refregier, A., Rhodes, J., & Groth, E. J. 2002, ApJ, 572, L131

- Schneider, P. 1998, *ApJ*, 498, 43
- Schneider, P., van Waerbeke, L., Jain, B., & Kruse, G. 1998, *MNRAS*, 296, 873
- Schneider, P., van Waerbeke, L., & Mellier, Y. 2002, *A&A*, 389, 729
- Somerville, R. S., Lemson, G., Sigad, Y., Dekel, A., Kauffmann, G., & White, S. D. M. 2001, *MNRAS*, 320, 289
- Strauss, M. S., & Willick, J. A. 1995, *Phys. Rep.*, 261, 271
- Tegmark, M., & Bromley, B. C. 1999, *ApJ*, 518, L69
- van Waerbeke, L. 1998, *A&A*, 334, 1
- van Waerbeke, L., et al. 2001, *A&A*, 374, 757
- van Waerbeke, L., Mellier, Y., Pello, R., Pen, U.-L., McCracken, H. J., & Jain, B. 2002, *A&A*, in press
- Verde, L., et al. 2001, *MNRAS*, submitted (astro-ph/0112161)
- Wilson, G., Kaiser, N., & Luppino, G. A. 2001, *ApJ*, 556, 601
- Yee, H. K. C., et al. 2000, *ApJS*, 129, 475
- Yee, H. K. C., & Gladders, M. D. 2001, in *ASP Conf. Ser. 257, AMiBA 2001: High-z Clusters, Missing Baryons, and CMB Polarization*, ed. L.-W. Chen et al. (San Francisco: ASP), in press
- Yoshikawa, K., Taruya, A., Jing, Y. P., & Suto, Y. 2001, *ApJ*, 558, 520